FMEA-Based Risk Index method and Predictive Rule for Assessing Monorail Crane Stability*

Bohdan Solovei[1,*,†] and Oleksandr Terentyev[1,†]

[1] Kyiv National University of Construction and Architecture, 31, Air Force Avenue, Kyiv, 03037, Ukraine

Abstract

This research enhances the operational safety of mobile monorail cranes by developing a novel method for quantifying stability loss risk and a predictive rule for generating timely warnings. A review of existing literature reveals a gap: while many studies enhance Failure Mode and Effects Analysis (FMEA), they do not integrate predictive neural network models for forecasting physical stability coefficients. This research directly addresses this gap by proposing an approach where recurrent neural networks predict crane stability coefficients. These predictions are then synthesized into a new, validated risk index based on FMEA principles. The study's tasks include: a novel risk index that quantifies stability loss by calculating Severity (S), Occurrence (O), and Detectability (D); a predictive rule for signaling potential stability loss; a validation of both the index and the rule. The results confirm the risk index's physical consistency, evidenced by logical correlations between its components ($\rho(S, O) = 0.81$; $\rho(S, D) = -0.78$; $\rho(O, D) = -0.96$). The validation confirmed the rule's predictive capability, showing that it generates warning signals before a hazardous state occurs. These validated components are designed to serve as the core of a future monorail crane stability monitoring system.

Keywords

Recurrent Neural Networks, predictive modeling, FMEA, risk assessment, safety monitoring, monorail crane

1. Introduction

The stability of a mobile monorail crane is a complex, dynamic state influenced by a confluence of factors, including payload characteristics, boom geometry, ground conditions, and environmental variables such as wind gusts. This com-plexity makes traditional, static safety checks insufficient for ensuring opera-tional safety in real time.

In study [1], the effectiveness of two neural network architectures for mono-rail crane monitoring was investigated separately: a multitask Gated Recurrent Unit (GRU) with a self-attention mechanism and a multitask GRU with a Bayesi-an attention mechanism. The conclusions recommend combining predictions from the deterministic recurrent neural networks GRU architecture with self-attention and the Bayesian architecture in crane stability monitoring systems.

However, existing risk assessment methods for crane stability monitoring ei-ther focus on enhancing FMEA logic without leveraging real-time predictive data or analyzing system dynamics without translating them into a formal FMEA-based risk index and actionable alert system.

This paper addresses this gap by proposing a novel methodology for the pre-dictive assessment of monorail crane stability. The proposed approach is based on two innovations. First, multitask GRU neural networks are employed to gener-ate real-time forecasts of the crane's physical stability coefficients for overturn-ing and sliding. Second, these predictions are synthesized into a dynamic risk index grounded in FMEA principles, quantifying risk through three components: Severity (S),

* The Third International Conference of Young Scientists on Artificial Intelligence for Sustainable Development: Intelligent Systems and Artificial Intelligence (YAISD-WS 2026:ISAI) May 7-8, 2026, Ternopil, Ukraine

1,* Corresponding author.

† These authors contributed equally.

controlerrf5@gmail.com (B. Solovei); terentiev.oo@knuba.edu.ua(O. Terentyev);

0009-0008-0328-1123 (B. Solovei); 0000-0001-6995-1419 (O. Terentyev);

© 2026 Copyright for this paper by its authors. Use permitted under Creative Commons License Attribution 4.0 International (CC BY 4.0).

CEUR Workshop Proceedings ceur-ws.org ISSN 1613-0073

published 2026-11-11

CEUR-WS.org/Vol-4326/paper3.pdf

Occurrence (O), and Detectability (D). Based on this index, a com-posite logical rule is designed and validated to generate timely signals of poten-tial instability.
The primary objective of this research is therefore to enhance operational safety of a mobile monorail crane by developing a predictive system capable of quantifying the risk of stability loss and warning operators before a hazardous state occurs.

2. Research Objectives

The goal of this research is to enhance the operational safety of mobile monorail cranes.
To achieve this objective, the study addresses the following tasks:
1. Develop a novel risk index calculation method for the stability loss risk of a monorail crane, based on FMEA principles.
2. Design a rule for generating a signal of potential stability loss risk.
3. Validate the proposed risk index calculation method and the signal-generation rule for potential stability loss.

3. Literature Review

The approaches which enhance the traditional FMEA for building crane risk assessment can be grouped into three categories: modifications of FMEA to handle uncertainty; probabilistic risk models with factor coupling, and dynamic functional risk models.
The first group includes studies [2–5], which focus on improving FMEA under uncertainty. In [2], subjective weights obtained via the Analytic Hierarchy Process (AHP) are combined with objective weights from the Step-wise Weight Assessment Ratio Analysis method into a unified weighting scheme, enhancing flexibility and reliability in uncertain conditions. Study [3] integrates Z-number theory and Set Pair Analysis (SPA) within FMEA, allowing expert judgments with uncertainty to be transformed and aggregated for comprehensive risk evaluation. In [4], a hybrid fuzzy multi-criteria decision-making approach combines FMEA, FSWARA, and FWASPAS to identify, evaluate, and rank risks, addressing uncertainty and subjectivity in construction projects. Study [5] proposes an advanced FMEA framework integrating probabilistic linguistic term sets (PLTS), the Fuzzy Best–Worst Method (FBWM), load-sharing modeling, and TOPSIS. This approach quantifies expert judgments, models failure propagation, and improves risk prioritization by combining subjective and objective data.
The second group is represented by [6], which integrates Bayesian Networks (BN) with the N-K model to analyze coupling effects among risk factors. The N-K model defines the structure and degree of interactions, showing that risk increases with the number of coupled factors. These relationships are incorporated into a BN, enabling probabilistic causal analysis beyond traditional static RPN methods.
The third group, represented by [7], combines the Functional Resonance Analysis Method (FRAM) with Bayesian Networks to model functional variability and probabilistic dependencies in crane operations. FRAM identifies system functions and their interactions, while Monte Carlo simulations quantify variability. The resulting risks are incorporated into a BN, enabling integrated static and dynamic risk assessment.
Overall, the first group focuses on uncertainty handling and multi-criteria aggregation but does not employ neural network-based prediction. The second and third groups address probabilistic causality, coupling, and functional variability, yet do not utilize neural networks for predicting physical stability coefficients or calculating risk indices. None of the reviewed studies combines neural network-based physical predictions with FMEA-style risk components and composite logical rules for risk signal generation in crane stability assessment.

4. Materials and Methods

4.1. Risk Index calculation method for stability loss risk of the monorail cran

Let at time t the predicted estimates of the stability coefficients for overturning β(t) and sliding γ(t) of the monorail crane be obtained as the outputs of two multitask recurrent GRU neural networks. Let τ∈{β,γ} defines the type of monorail crane stability coefficient.

The GRU network with a self-attention mechanism produces deterministic forecasts of the mean values [9]:

$$\hat{\beta}_1(t)=\mu_{1,\beta}(t),\hat{\gamma}_1(t)=\mu_{1,\gamma}(t) \tag{1}$$

where $\hat{\beta}_1(t),\hat{\gamma}_1(t)$ denotes predicted by GRU with a self-attention mechanism the stability coefficients of the monorail crane; $\mu_{1,\beta}(t)$, $\mu_{2,\gamma}(t)$ denotes the predicted by GRU with a self-attention mechanism the mean value of the stability coefficients.

The GRU network with an attention mechanism and Bayesian approximation produces the parameters of a normal distribution [10]:

$$\hat{\beta}_2(t)\sim N(\mu_{2,\beta}(t),\sigma^2_{2,\beta}(t)),\hat{\gamma}_2(t)\sim N(\mu_{2,\gamma}(t),\sigma^2_{2,\gamma}(t)) \tag{2}$$

where $\mu_{2,\beta}(t)$, $\mu_{2,\gamma}(t)$ denotes the predicted by GRU with an attention mechanism and Bayesian approximation mean value of the stability coefficients, while $\sigma_{2,\beta}(t)$, $\sigma_{2,\gamma}(t)$ represents the uncertainty of the forecast.

The probability of violating the safe state O(t) is defined as the probability ($p_{fail,\tau}(t)$) of an unsafe state based on the predictions of the GRU model with a self-attention mechanism [11]:

$$p_{\text{fail},\tau}(t)=\Phi\left(\frac{\theta_\tau-\mu_{1,\tau}(t)}{\sigma_{\theta,\tau}}\right), \tag{3}$$

where:

$\Phi(z)=\frac{1}{2}\left(1+erf\left(\frac{z_1}{\sqrt{2}}\right)\right)$ - is the cumulative distribution function (CDF) of the standard normal distribution; $z_1=\frac{\theta_\tau-\mu_{1,\tau}(t)}{\sigma_{\theta,\tau}}$ is a standard normal variable; erf(·) denotes the error function, defined as: $erf(x)=\frac{2}{\sqrt{\pi}}\int_0^x e^{-t^2}dt$, x∈R [12].

θ_τ denotes the threshold values of the stability coefficients for overturning (θ_β) and sliding (θ_γ) of the monorail crane. $\theta_\beta\geq1.4$ corresponds to the minimum safety factor ensuring sufficient reserve against overturning moments; $\theta_\gamma\geq1.5$ corresponds to the minimum safety factor ensuring robustness against surface irregularities, dynamic load variations [13].

$\sigma_{\theta,\tau}$ - represents the upper bound of the permissible uncertainty interval for assessing stability: for overturning [15%, 20%]· θ_β, and for sliding [15%, 20%]· θ_γ.

The severity component S(t) is defined based on the conditional expectation in the dangerous tail of the predictive distribution of the Bayesian model, which allows estimating the consequences of a potential violation [14].

Let $\hat{y}_\tau(t)$ be the predicted stability coefficient for mode τ∈{β,γ} at time t: $\hat{y}_\tau(t)\sim N(\mu_{2,\tau}(t),\sigma^2_{2,\tau}(t))$. To ensure numerical stability (when σ⟶0), a lower bound $\sigma'_{2,\tau}(t)=max(\sigma_{2,\tau}(t),\varepsilon)$ is considered in the denominator of standard normal variable $z_2=\frac{\theta_\tau-\mu_{2,\tau}(t)}{\sigma'_{2,\tau}(t)}$.

The expected value of the predicted stability coefficient under the condition that it lies in unsafe region $\hat{y}_\tau(t) < \theta_\tau$ is given by:

$$E\left[\hat{y}_\tau(t) \mid \hat{y}_\tau(t) < \theta_\tau\right] = \mu_{2,\tau}(t) - \sigma'_{2,\tau}(t)\frac{\varphi\left(z_{2,\tau}(t)\right)}{\Phi\left(z_{2,\tau}(t)\right)} \tag{4}$$

where φ(·) is the probability density function (PDF) of the standard normal distribution; $\Phi(\cdot)$ is the cumulative distribution function (CDF) of the standard normal distribution; $\frac{\varphi\left(z_{2,\tau}(t)\right)}{\Phi\left(z_{2,\tau}(t)\right)}$ is the lower-tail inverse Mills ratio [15].

The normalized deficit is defined as:

$$u_\tau(t) = min\left(1, \frac{\sigma'_{2,\tau}(t)}{\sigma_{\theta,\tau}}\right) \tag{5}$$

According to (5) when $\mu_{2,\tau}(t) \ll \theta_\tau$ then $\Phi\left(z_\tau(t)\right) \to 1$ so $\frac{\varphi\left(z_\tau(t)\right)}{\Phi\left(z_\tau(t)\right)} \to 0$; $E[\cdot] \approx \mu$ and $s_\tau(t)$ increases; when $\mu_{2,\tau}(t) \gg \theta_\tau$ then $\Phi\left(z_\tau(t)\right) \to 0$ so $\frac{\varphi\left(z_\tau(t)\right)}{\Phi\left(z_\tau(t)\right)} \to \infty$; $E[\cdot] \to \theta$ and $s_\tau(t)$ decreases.

The detectability component D(t) is defined through the normalized uncertainty of the Bayesian model [16]:

$$s_\tau(t) = min\left(1, max\left(0, \frac{\theta_\tau - E\left[\hat{y}_\tau(t) \mid \hat{y}_\tau(t) < \theta_\tau\right]}{\theta_\tau}\right)\right) \tag{6}$$

$$u_\tau(t) = min\left(1, \frac{\sigma'_{2,\tau}(t)}{\sigma_{\theta,\tau}}\right) \tag{7}$$

Aggregated FMEA scores in the range [1,10] is defined as

$$O(t) = 1 + 9 \cdot \frac{p_{fail,\beta}(t) + p_{fail,\gamma}(t)}{2} \tag{8}$$

$$S(t) = 1 + 9 \cdot \frac{s_\beta(t) + s_\gamma(t)}{2} \tag{9}$$

$$D(t) = 1 + 9 \cdot \frac{u_\beta(t) + u_\gamma(t)}{2} \tag{10}$$

The normalized risk index is defined as

$$R(t) = \frac{S(t) + O(t) + D(t) - 3}{27} \tag{11}$$

where R(t)∈[0,1].

4.2. A rule for generating a signal of potential stability loss risk of the monorail crane

A rule for generating a signal of potential stability loss risk of the monorail crane is proposed based on a composition of triggers.

Trigger for stability coefficient violation:

$$A_1 = \left(\hat{\beta}_1 < \theta_\beta\right) \vee \left(\hat{\gamma}_1 < \theta_\gamma\right) \tag{12}$$

where θ_β=1.4, θ_γ =1.5 - limit values of the overturning and sliding stability coefficients of the monorail crane, respectively.

Trigger for exceeding permissible forecast uncertainty:

$$A_2 = \left(\sigma_{2,\beta} > \sigma_{\theta,\beta}\right) \vee \left(\sigma_{2,\gamma} > \sigma_{\theta,\gamma}\right) \tag{13}$$

where $\sigma_{\theta,\beta}$=0.28, $\sigma_{\theta,\gamma}$=0.3 - upper bound of the permissible uncertainty interval for assessing stability calculated for overturning [15%...20%]· $\theta_\beta \approx$[0.21…0.28], and for sliding [15%...20%]· $\theta_\gamma \approx$[0.225…0.3].

Trigger for exceeding the integrated risk threshold:

$$A_3 = R(t) > \theta_R \tag{14}$$

The composite predictive rule is defined as

$$A = A_1 \wedge (A_2 \vee A_3) \tag{15}$$

The logical rule (14) generates a risk signal when the predicted violation of the limit state is detected and at least one additional condition is satisfied: excessive forecast uncertainty or exceeding the integrated risk threshold.

4.3. Approach to validate the proposed risk model and the rule

The structure of the risk model (14) is considered physically consistent if the following conditions are satisfied (Fig.1.):

1. The absolute values of Spearman's rank correlation coefficients must exceed 0.5, which corresponds to a strong monotonic relationship [17]:

$$H_0 = |\rho| \le 0.5 \; H_1 = |\rho| > 0.5 \tag{16}$$

H_1 is accepted if $CI_{95\%(\rho)} \subset (-1,-0.5) \cup (0.5,1)$.

2. The signs of the correlations correspond to the expected structural dependence of the risk components:

$$\rho(S,O) > 0 \wedge \rho(O,D) < 0 \wedge \rho(S,D) < 0. \tag{17}$$

3. A structural index is used for the integral assessment of the consistency of the component structure:

$$SCI = \frac{|\rho(S,O)| + |\rho(O,D)| + |\rho(S,D)|}{3} > 0.7 \quad (18)$$

To verify that the components S(t), O(t), and D(t) reflect different aspects of the technical condition of the system, an analysis of their temporal evolution to be performed. The verification algorithm includes the following steps:

1. Construct time series for the components S(t), O(t), and D(t).
2. Determine the range of values for each component.
3. Check that each component demonstrates variation over time and responds to changes in the system state.

If the components exhibit different dynamics and different scales of value variation, it is considered that they reflect different aspects of risk.

To verify the selection of the threshold value for the integrated risk index θ_R, a sensitivity analysis of the logical rule (14) to be performed. The verification algorithm includes the following steps:

Construct the dependence of the number of risk signals $N(\theta_R) = \sum_t 1\{Action_{\theta_R}(t) = 1\}$ on the threshold value of the integrated risk index θ_R.

1. Determine the interval of θ_R values where the greatest change in the number of signals is observed.
2. Select the operating threshold value θ_R from this interval.

To verify the structure of the proposed rule (14), an analysis of the role of individual triggers within rule (14) to be performed. The verification algorithm includes the following steps:

1. Calculate the number of activations for each trigger: $\sum_t A_1(t)$, $\sum_t A_2(t)$, $\sum_t A_3(t)$.
2. Calculate the number of their unique activations:

A_1 only: $A_1 \wedge \neg A_2 \wedge \neg A_3$,

A_2 only: $A_2 \wedge \neg A_1 \wedge \neg A_3$,

A_3 only: $A_3 \wedge \neg A_1 \wedge \neg A_2$.

If a risk signal is generated only when the composition of triggers is satisfied according to rule (14), then such a rule ensures the generation of warning signals regarding the potential loss of stability of the monorail crane.

To verify that the proposed risk index method correctly ranks system states according to the level of stability loss risk, a rank-consistency analysis between the integrated risk index R(t) and the physical stability margin m(t) is performed. The verification algorithm includes the following steps:

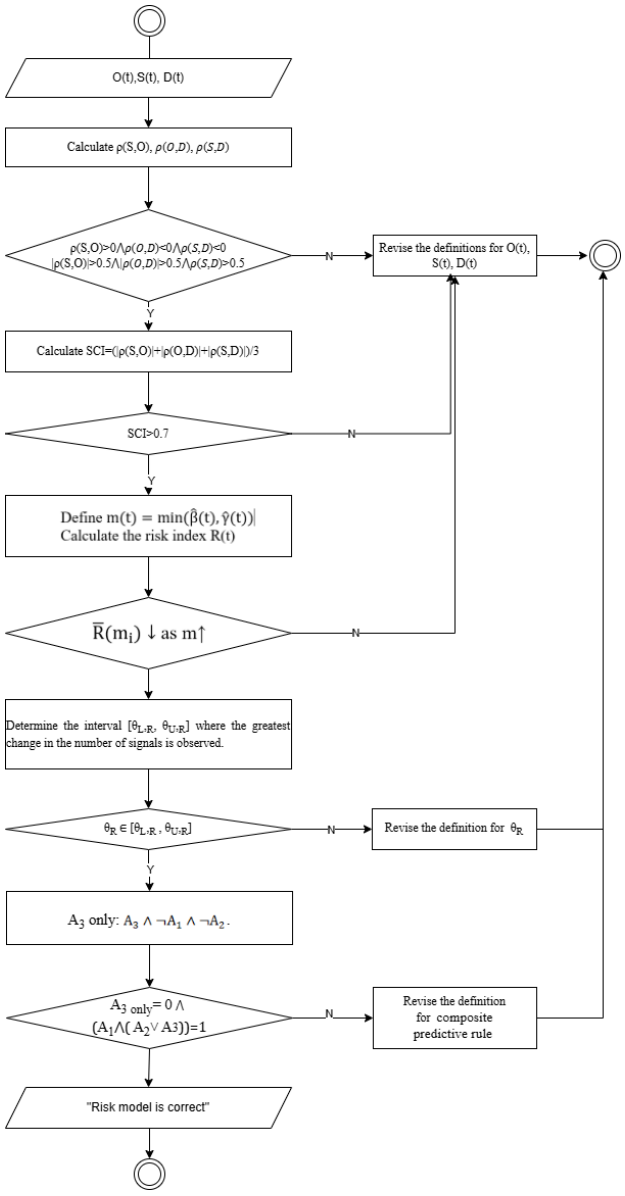


Figure 1: Risk model validation flow.

1. Define the stability margin of the system: $m(t)=min(\hat{\beta}(t),\hat{\gamma}(t))$. Lower values of m(t) correspond to states closer to the stability limit and therefore represent higher physical risk.
3. Calculate the risk index R(t) according to equation (10) for all time steps t.
4. Compute the Spearman rank correlation coefficient between the stability margin and the risk index: ρ(m,R).
5. Plot the dependence between R(t) and m(t) in order to visually analyze the relationship between the stability margin and the risk index.
6. Divide the range of m(t) into intervals and calculate the mean value of the risk index in each interval: $\overline{R}(m_i)$ together with the corresponding 95% confidence intervals.
7. Check that the mean value of the risk index decreases with increasing stability margin: $\overline{R}(m_i)\downarrow$ as m↑.

If the Spearman correlation coefficient satisfies the condition ρ(m,R)<0 and the binned analysis demonstrates a monotonic decrease of the average risk index with increasing stability margin, then the proposed risk index is considered rank-consistent with the physical stability margin of the crane.

5. Experiment Setup

The proposed approach for assessing the stability risk of the monorail crane was applied to the output forecasts of the multitask GRU with a self-attention mecha-nism and a multitask GRU with a Bayesian attention mechanism developed in [1]. Dataset for experiments was created according to the approach designed and verified in [18]. The proposed risk index calculation method developed using the Python programming language in the following software environment: NumPy (version 2.2.4), Math, Pandas (version 2.2.3), Scikit-learn (version 1.6.1), Mat-plotlib (version 3.10.1). The results of its application, as well as the results of the consistency check of the risk index calculation method and the rules, are pre-sented in the following section.

6. Results and Discussion

Figure 2 presents the matrix of Spearman's rank correlation coefficients between the risk components S, O, and D, as well as the estimates of the corresponding coefficients with 95% confidence intervals. A strong positive relationship is observed between the severity of consequences and the probability of failure components: $\rho(S, O) = 0.81$, $CI_{95\%(\rho(S,\ O))} = [0.74; 0.867]$. The confidence interval lies entirely within the range (0.5, 1), which allows for the acceptance of the alternative hypothesis H_1 according to condition (15). The positive sign of the correlation is consistent with the expected structural dependence (16): as the probability of exceeding the limit state increases, the severity of consequences also increases. For the pair of severity of consequences and risk detectability components, a strong negative relationship is observed: $\rho(S, D) = -0.78$, $CI_{95\%(\rho(S,\ D))} = [-0.853; -0.694]$. The interval is entirely within $(-1, -0.5)$, which also confirms the acceptance of hypothesis H_1. The negative sign of the correlation indicates that as the severity of potential consequences increases, the detectability index decreases, which is consistent with the interpretation of component D as a characteristic of forecast uncertainty. The strongest relationship is observed between the probability of failure and risk detectability components: $\rho(O, D) = -0.96$, $CI_{95\%(\rho(O,\ D))} = [-0.967; -0.646]$. The narrow confidence interval and the large absolute value of the coefficient indicate an extremely strong negative monotonic relationship between these indicators. This dependence means that as the probability of a hazardous state increases, the D index decreases, which corresponds to the logic of the metric construction (8).

Thus, for all three pairs of components, the condition of strong association $|\rho| > 0.5$ is satisfied, and the signs of the coefficients correspond to the expected structural scheme (16). Based on the obtained values, the structural consistency index can be calculated: $SCI = (|0.81| + |-0.96| + |-0.78|) / 3 \approx 0.85$. Since $SCI > 0.7$, condition (17) is also satisfied. Therefore, the results of the statistical analysis confirm the physical consistency of the proposed risk structure (10). The obtained dependencies between the S, O, and D components correspond to the expected engineering interpretation and indicate the correctness of the risk index formalization for assessing the loss of stability of the monorail crane.

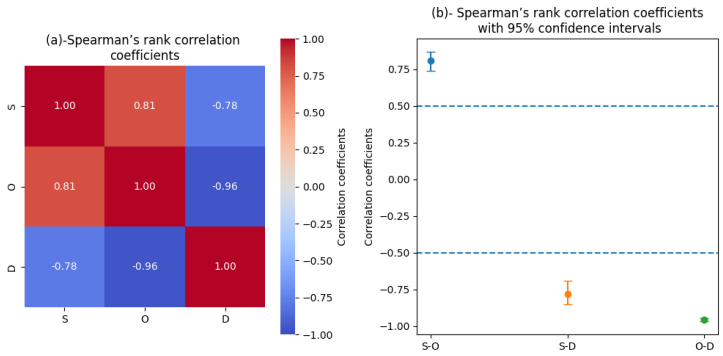


Figure 2: Statistical analysis: (a) matrix of Spearman's rank correlation coefficients between the risk components S, O, and D; (b) 95% confidence intervals for Spearman's correlations between the risk components S, O, and D.

Figure 3(a) shows the temporal evolution of the risk components S(t), O(t), and D(t). The results indicate that S(t) values are mainly in the range 1.7–4, which indicates relatively moderate severity of consequences in most cases. The O(t) component demonstrates a wider range of variation (approximately 1.5–9), corresponding to different levels of probability of stability loss. The D(t) index varies in the range of approximately 5–10, reflecting the influence of uncertainty in the Bayesian model forecasts.

Figure 3(b) presents the results of the sensitivity analysis of the logical rule (14) to the selection of the threshold value of the integrated risk index θ_R. The obtained dependence demonstrates a monotonic decrease in the number of risk signals as the threshold value increases. In the range $\theta_R <$ 0.45, the system generates approximately 145–150 signals, while for $\theta_R >$ 0.45, the number of activations stabilizes at about 23.

Thus, the results of the component dynamics analysis show that the indicators S(t), O(t), and D(t) respond to changes in the stability state of the monorail crane. The sensitivity analysis of the threshold value θ_R shows a monotonic decrease in the number of risk signals with increasing threshold, confirming the controllability of the proposed logical rule. The greatest change in the number of signals is observed in the range $0.45 \le \theta_R \le 0.6$, which allows for the determination of the operating threshold value based on sensitivity analysis.

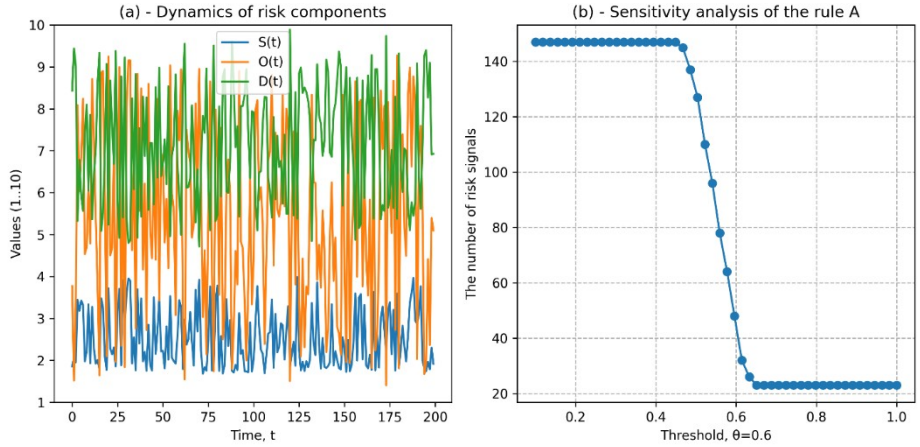


Figure 3: Dynamics of risk components and sensitivity of the logical rule: (a) time series of the components S(t), O(t), D(t); (b) dependence of the number of risk signals on the threshold value of the integrated risk index θ_R.

Figure 4 presents the results of the analysis of the frequency of activation of individual triggers of the logical rule. On Fig. 4(a) - the total number of activations of the limit state violation trigger A_1 is 147 cases, which is the highest among all components. The trigger for exceeding the permissible level of uncertainty A_2 is activated in 56 cases, while the exceedance of the integrated risk index A_3 is observed in about 20 cases. The analysis of unique activations on Fig. 4(b) shows that 104 cases are associated exclusively with trigger A_1, while 33 cases are due only to exceeding the permissible level of uncertainty. At the same time, isolated activations of trigger A_3 are absent.

The obtained results indicate that the proposed logical rule (14) is activated before the occurrence of an emergency situation, i.e., it is a predictive rule for determining the risk of loss of stability of the monorail crane.

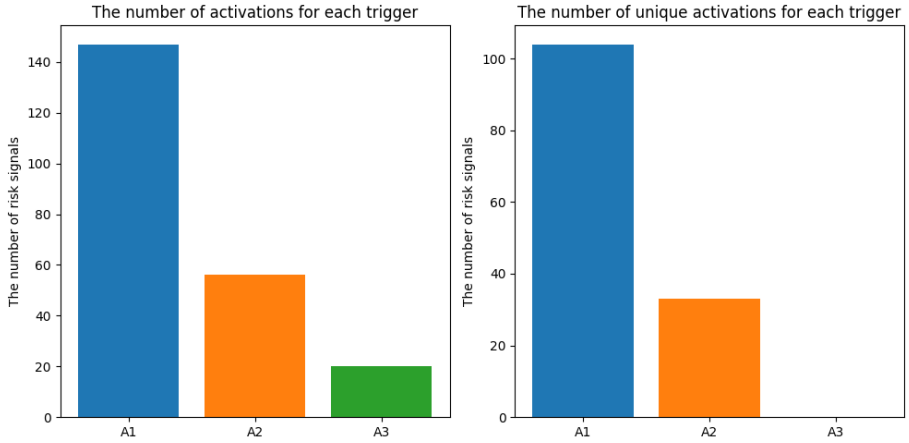


Figure 4: Decomposition of the frequency of trigger activations of the logical rule for risk signal determination: (a) total number of activations for each trigger; (b) number of unique activations.

Figure 5 illustrates dependence of the integrated risk index R(t) on the crane's stability margin m(t). Fig. 5(a) shows the scatter plot of the relations between R(t) and m(t) = min(β, γ). A strong negative rank correlation is obtained, ρ = −0.891, indicating an increase in the risk index as the stability margin decreases. Fig. 5(b) presents the dependence of the mean risk index value in intervals of m(t). A monotonic trend of decreasing R with increasing stability margin is observed.

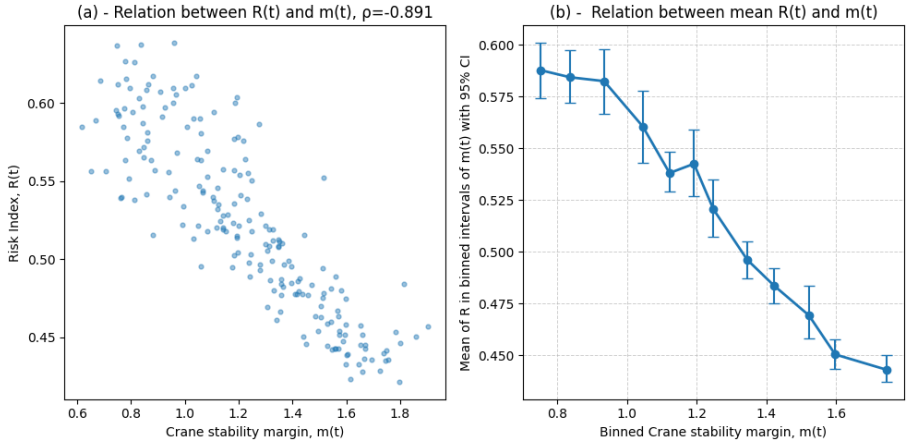


Figure 5: Dependence of the integrated risk index on the crane's stability margin: (a) - the relations between R(t) and m(t) = min(β, γ); (b) - mean value of R in binned intervals of m(t) with 95% confidence intervals.

Conclusions

This research's goal is to enhance the operational safety of mobile monorail cranes by developing a novel risk index method for quantifying stability loss risk and a predictive rule for generating timely warnings.

A new risk index calculation method for the stability loss risk of the monorail crane was proposed and validated. This method, grounded in FMEA principles, integrates predictions from GRU neural networks to calculate Severity (S), Oc-currence (O), and Detectability (D) components. The validation confirmed the method has physical consistency, demonstrating the correlations between its components (ρ(S, O) = 0.81; ρ(S, D) = −0.78; ρ(O, D) = −0.96). The calculated Risk Index was proven to be rank-consistent with the crane's physical stability margin (ρ = −0.891).

The paper proposed a rule for generating a signal of potential stability loss risk. This composite logical rule effectively combines triggers for predicted limit-state violations, excessive forecast

uncertainty, and high integrated risk levels. The validation of this rule confirmed its predictive capability, showing that it generates warning signals before a hazardous state occurs. Sensitivity analysis demonstrated the rule's controllability and identified an optimal threshold range ($0.45 \leq \theta R \leq 0.6$) for its application.

The results confirm the successful accomplishment of research's tasks.

Future research will focus on designing the architecture of a monorail crane stability monitoring system that incorporates the proposed and validated risk index calculation method and the signal-generation rule as core methodological components.

Declaration on Generative AI

The author(s) have not employed any Generative AI tools.

References

[1] O. Terentyev, B. Solovei, Multitask recurrent neural network architectures for information technology-based safety monitoring of a monorail crane, Herald of Khmelnytskyi National University. Technical Sciences 363(2) (2026) 576–586. doi:10.31891/2307-5732-2026-363-76

[2] K. H. Chang, T. Y. Fang, Z. S. Li, Using a flexible risk priority number method to reinforce abilities of imprecise data assessments of risk assessment problems, Electronics 14 (2025) 518. doi:10.1016/j.heliyon.2024.e28603.

[3] A. Li, Risk assessment of crane operation hazards using modified FMEA approach with Z-number and set pair analysis, Heliyon 10 (2024) e28603. doi:10.1016/j.heliyon.2024.e28603.

[4] A. Alvand, S. M. Mirhosseini, M. Ehsanifar, E. Zeighami, A. Mohammadi, Identification and assessment of risk in construction projects using the integrated FMEA-SWARA-WASPAS model under fuzzy environment: a case study of a construction project in Iran, International Journal of Construction Management 23 (2023) 392–404. doi:10.1080/15623599.2021.1877875.

[5] B. Sun, L. Wang, J. Zhang, N. Ding, Improved FMEA risk assessment based on load sharing and its application to a magnetic lifting system, Machines 13 (2025) 1113. doi:10.3390/machines13121113.

[6] B. J. Wu, L. H. Jin, X. Z. Zheng, S. Chen, Coupling analysis of crane accident risks based on Bayesian network and the NK model, Scientific Reports 14 (2024) 1133. doi:10.1038/s41598-024-51425-9.

[7] H. Zhong, L. Chen, M. F. Antwi-Afari, Z. Bao, K. Chen, Dynamic risk assessment of tower crane operations by integrating functional resonance analysis method and Bayesian network, Developments in the Built Environment 23 (2025) 100699. doi:10.1016/j.dibe.2025.100699.

[8] Y. Khosravi, F. Hosseinali, M. Adresi, Identifying accident prone areas and factors influencing the severity of crashes using machine learning and spatial analyses, Scientific Reports 14 (2024) 29836. doi:10.1038/s41598-024-81121-7.

[9] S. Jung, J. Moon, S. Park, E. Hwang, An attention-based multilayer GRU model for multistep-ahead short-term load forecasting, Sensors 21 (2021) 1639. doi:10.3390/s21051639.

[10] Y. Chen, W. Guan, R. Azzam, Residual Bayesian attention networks for uncertainty quantification in regression tasks, Scientific Reports 15 (2025) 38279. doi:10.1038/s41598-025-24093-6.

[11] Z. Chen, X. Yan, L. Wang, Q. Luo, Y. Yan, T. Qiu, P. Cheng, Research on reliability index and failure probability of inherent defect insurance from the insurance perspective, Heliyon 10 (2024). doi:10.1016/j.heliyon.2024.e26160.

[12] Wikipedia, Fundamental theorem of calculus, in: Wikipedia, the free encyclopedia. URL: https://en.wikipedia.org/wiki/Fundamental_theorem_of_calculus#Formal_statements. Last accessed: 2020/11/12.

[13] V. O. Volianiuk, Ye. V. Horbatiuk, Rozrakhunok mekhanizmiv vantazhopidiymalnykh mashyn, KNUBA, Kyiv, 2021.

[14] F. B. Hüttel, F. Rodrigues, F. C. Pereira, Deep evidential learning for Bayesian quantile regression, arXiv preprint arXiv:2308.10650 (2023). URL: https://arxiv.org/pdf/2308.10650.
[15] S. J. Haberman, Advanced statistics: Description of populations, Springer Science & Business Media, Heidelberg, 2013.
[16] P. J. van Leeuwen, J. Y. C. Chiu, C. K. K. Yang, Uncertainty quantification for deep learning, Environmental Data Science 4 (2025) e53. doi:10.1017/eds.2025.10027.
[17] P. Schober, C. Boer, L. A. Schwarte, Correlation coefficients: appropriate use and interpretation, Anesthesia & Analgesia 126 (2018) 1763–1768. doi:10.1213/ANE.0000000000002864.
[18] B. Solovey, O. Terentyev, An approach to generating physically realistic data for crane safety monitoring systems based on finite element modeling, Innovative Technologies and Scientific Solutions for Industries 1(35) (2026) 115–126. doi:10.30837/2522-9818.2026.1.115.